

# Redox-active Magnetic Resonance Imaging Contrast Agents: Studies with Thiol-bearing 1,4,7,10-Tetraazacyclododecane-1,4,7,10-tetracetic Acid Derivatives

Bhumasamudram Jagadish,<sup>†</sup> Gerald P. Guntle,<sup>‡</sup> Dezheng Zhao,<sup>‡</sup> Vijay Gokhale,<sup>§</sup> Tarik J. Ozumerzifon,<sup>†</sup> Ali M. Ahad,<sup>†</sup> Eugene A. Mash,<sup>†</sup> and Natarajan Raghunand<sup>\*,‡,||</sup>

<sup>†</sup>Department of Chemistry and Biochemistry, University of Arizona, Tucson, Arizona 85721-0041, United States

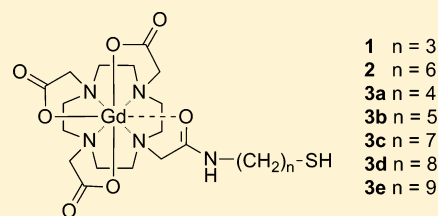
<sup>‡</sup>Arizona Cancer Center, University of Arizona, Tucson, Arizona 85724-5024, United States

<sup>§</sup>Department of Pharmacology and Toxicology, University of Arizona, Tucson, Arizona 85721-0240, United States

<sup>||</sup>Department of Radiology, University of Arizona, Tucson, Arizona 85724-5067, United States

## S Supporting Information

**ABSTRACT:** The synthesis and structure–activity relationships of a homologous series of 1,4,7,10-tetraazacyclododecane-1,4,7,10-tetracetic acid gadolinium(III) complexes bearing thiol-terminated alkyl side chains from three to nine carbons in length are reported. The observed binding with human serum albumin (HSA) of the compounds having C-3 through C-7 side chain lengths was inhibited by homocysteine in a manner consistent with single-site binding. The observed binding with HSA of the compounds having C-8 and C-9 side chain lengths was only partly inhibited by homocysteine, consistent with multisite binding. The binding affinity of the C-7 compound could be related to the HSA oxidation state. 2D <sup>1</sup>H–<sup>1</sup>H NMR TOCSY provided evidence of covalent binding of the europium analog of the C-6 compound to HSA-Cys<sup>34</sup>. The longitudinal water-proton MRI relaxivities of the gadolinium complexes at 7 T increased upon binding to HSA. On the basis of these results, the C-6 and C-7 compounds were identified as promising redox-sensitive MRI contrast agents.



## INTRODUCTION

In vivo results indicate that the redox state of thiol/disulfide pools in human plasma varies little between healthy individuals, and in vitro both cultured cells and perfused tissues are able to regulate the extracellular redox state.<sup>1</sup> In mammalian cells, response to oxidative stress is brought about by the nuclear factor erythroid 2-related factor 2 (NRF2) transcription factor, which is normally sequestered in the cytoplasm by Kelch-like ECH-associated protein 1 (KEAP1). In response to oxidative stress, NRF2 dissociates from KEAP1 and activates transcription of many protective genes, including genes for glutathione synthesis and genes that encode for proteins such as glutathione reductase, thioredoxin, thioredoxin reductase, peroxiredoxin, and sulfiredoxin that restore oxidized intracellular thiols to their reduced states. NRF2 also controls the expression of the multidrug resistance protein (MRP), a putative glutathione transporter, thereby providing cells with the ability to control both intracellular and extracellular redox states in response to oxidative stress.<sup>2</sup> In vivo, plasma albumin exerts a buffering action on redox states of plasma thiols. Perturbation of thiol/disulfide balance is a feature of many pathological states, especially inflammatory diseases such as multiple sclerosis.<sup>3</sup>

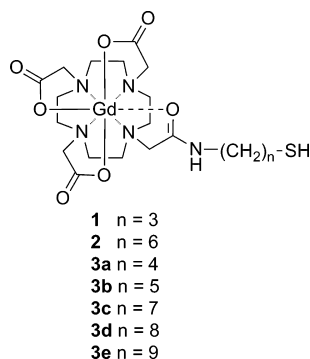
Reduced thiols can negatively impact the antitumor activities of platinum drugs, nitrogen mustards, doxorubicin, and nitrosoureas by conjugation to electrophilic groups on the

drug molecules.<sup>4</sup> Elevated expression of the gene targets of NRF2 has been implicated in chemoresistance in ovarian cancer cells in vitro.<sup>5</sup> Elevated cellular thiol concentrations have also been reported to diminish radiation response by scavenging intracellular ROS produced by ionizing radiation.<sup>6</sup> Contrarily, reduced glutathione and *N*-acetylcysteine have been shown to inhibit the activation and function of MMP-9, a matrix metalloproteinase implicated in the malignant progression of precancerous lesions, by preserving the cysteine sulfur blockage of the active site in the pro-peptide.<sup>7</sup> The physiological nonprotein thiols (NPSH) cysteine, homocysteine, and glutathione (GSH) have been reported to cause inactivation of transforming growth factor- $\beta$ , which can induce epithelial-to-mesenchymal transition of cells in late-stage tumors and promote tumor growth and metastasis.<sup>8</sup> Satoh, et al. have revealed a different mechanism by which NRF2 can play a role in the prevention of cancer metastasis, through its ability to preserve the redox balance in the hematopoietic and immune systems.<sup>9</sup> Thus, high levels of tumor NPSH may influence both cancer progression and tumor response to therapies, but toward opposing clinical outcomes. This highlights the need for noninvasive techniques for measuring tumor redox in vivo.

Received: May 26, 2012

Published: November 13, 2012

Previously we reported the synthesis of 1,4,7,10-tetraazacyclododecane-1,4,7,10-tetraacetic acid (DOTA) monoamide gadolinium(III) complexes **1** and **2** which bear propyl and hexyl side chains that terminate with a thiol group.<sup>10</sup> Complexes **1** and **2** bound to HSA in a demonstrably redox-sensitive manner. Recently the utility of **2** as a Magnetic Resonance Imaging (MRI) biomarker of tumor response to redox-active drugs in mice was demonstrated.<sup>11</sup> We also prepared DO3A gadolinium(III) complexes (not shown) possessing different ring nitrogen-attached side chains that also terminate with a thiol group.<sup>12</sup> Only one DO3A complex, bearing a 9-mercapto-3,6-dioxanonyl chain, bound in a redox-sensitive fashion. Other DO3A complexes additionally bound, we believe, to surface carboxylates of HSA. The DO3A complexes exhibited smaller longitudinal water proton relaxivities ( $r_1$ ) in both free and bound states than did the DOTA-monoamide complexes. This is presumably due to the displacement of water molecules from the DO3A complexes by acetate in the buffer in the free state and by surface carboxylates in the bound state. In a continuation of our work with Gd(III)-DOTA-monoamide complexes bearing thiol-terminated side chains, we have synthesized **3a–3e** that form a homologous series with **1** and **2**, studied the relationship of side chain length and binding to HSA, evaluated the relaxivity of these complexes in free and bound states, and used the europium analog of **2** in 2D NMR studies to probe binding of the complex to HSA at the Cys<sup>34</sup> site.



## RESULTS

**Synthesis.** The synthesis of gadolinium complexes **3a–3e** was accomplished by modification of our literature procedure (Scheme 1).<sup>10</sup> Phthalimides **5a–5e** were prepared in 81–93% yields by reaction of the known bromides **4a–4e**<sup>13–15</sup> with trityl mercaptan and sodium hydride in anhydrous DMF. Removal of the phthalimido groups in **5a–5e** with hydrazine hydrate in refluxing ethanol gave the amines **6a–6e** in 80–92% yields. Treatment of DOTA with isobutyl chloroformate, followed by addition of amines **6a–6e**, gave in 70–75% yields the corresponding tricarboxylic acids **7a–7e**. Reaction of **7a–7e** with Gd(OAc)<sub>3</sub> in refluxing water gave the Gd(III) complexes **8a–8e** in 85–94% yields. Finally, the trityl groups were removed with TFA/CH<sub>2</sub>Cl<sub>2</sub> (4% v/v) in the presence of Et<sub>3</sub>SiH, affording in 65–91% yields **3a–3e**.

The europium-loaded analog of **2** was synthesized starting from **9**<sup>10</sup> in two steps (Scheme 2). Reaction of **9** with Eu(OAc)<sub>3</sub> in refluxing water gave the Eu(III) complex **10** in 79% yield. Deprotection of the trityl group using TFA/CH<sub>2</sub>Cl<sub>2</sub> (4% v/v) in the presence of Et<sub>3</sub>SiH gave **11** in 79% yield. The

structures of all compounds, except **3a–3e**, **8a–8e**, **10**, and **11**, were characterized by chromatographic mobility, <sup>1</sup>H NMR, <sup>13</sup>C NMR, and HRMS. Compounds **3a–3e**, **8a–8e**, and **10** were characterized by chromatographic mobility and showed appropriate masses and isotopic patterns in HRMS analysis. Compound **11** was characterized by chromatographic mobility, <sup>1</sup>H NMR, and HRMS.

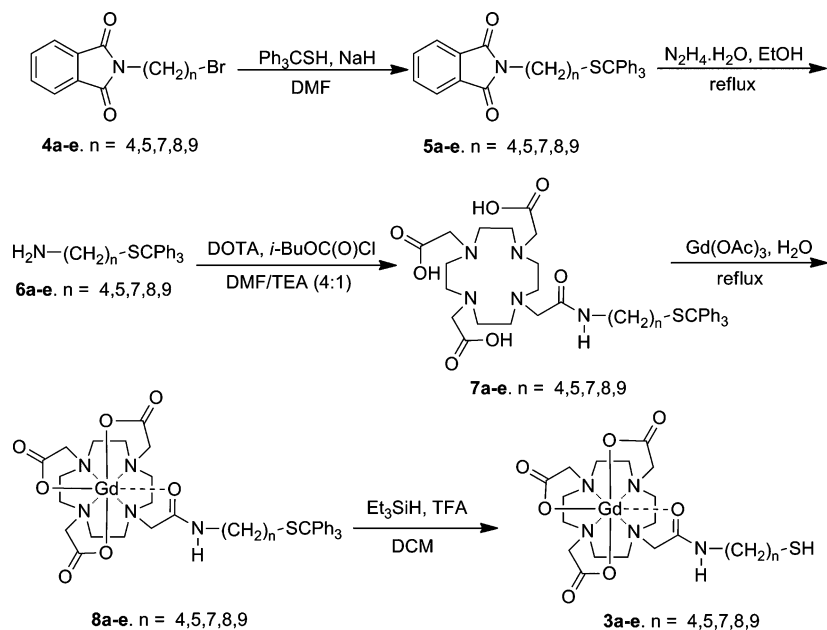
**Effect of Oxidation State of HSA on Binding Affinity of Complex 3c to Protein.** The binding of **3c** to protein was measured in phosphate-buffered saline (PBS) solutions that contained 0.6 mM recombinant HSA (rHSA, Invitria), recombinant lipid-reduced HSA (rHSA-LR, Invitria), HSA (Sigma), or mercapt-HSA (mHSA) prepared from HSA by the method of Jacobsen.<sup>16</sup> The thiol content of all four HSA preparations was assayed colorimetrically using Ellman's reagent (Figure 1).<sup>17</sup> While Ellman's reagent is known to react slowly and/or incompletely with thiols in undenatured proteins,<sup>18</sup> our results point to significant relative differences in thiol oxidation states between the four types of HSA.

The oxidation status of the Cys<sup>34</sup> residue in HSA would be expected to affect the binding of thiol-terminated Gd-DOTA-monoamide chelates. Figure 2 depicts the binding of **3c** to the four types of HSA in PBS as determined by the method described previously.<sup>12</sup> The calculated association constant ( $K_A$ ) for each HSA preparation correlates with the free thiol content of the protein. In addition, the bound fraction was below the theoretical maximum of one Gd per protein that would be expected for single-site binding. These findings are consistent with binding of **3c** to HSA at the Cys<sup>34</sup> residue.

**2D <sup>1</sup>H–<sup>1</sup>H NMR TOCSY Study of the Binding of Thiol-bearing Complex 11 to HSA.** Sadler and colleagues developed a model for structural changes in HSA upon binding of drugs to Cys<sup>34</sup>, whereby the Cys<sup>34</sup> moves from a buried to an exposed environment. They proposed that movement of Cys<sup>34</sup> is accompanied by movement of His<sup>3</sup>, which is part of the N-terminal segment of the protein, and have reported NMR methods for monitoring changes at His<sup>3</sup> upon binding of a drug to Cys<sup>34</sup>.<sup>19,20</sup> We used the europium-bearing complex **11** in 2D NMR studies to study binding of the complex to HSA. Compound **11** was incubated at 37 °C overnight with either HSA or mHSA in phosphate-buffered D<sub>2</sub>O saline, followed by freeze-drying and reconstitution in D<sub>2</sub>O for NMR spectroscopy. Deuterated solutions of HSA and mHSA without **11** were prepared analogously. All solutions contained sodium formate as the chemical shift reference (8.5 ppm). Consistent with Sadler's results for binding of the drug Auranofin at Cys<sup>34</sup>,<sup>19</sup> we observed changes in the splitting of the Hε1 resonance of the His<sup>3</sup> residue of HSA at ~8.2 ppm in 2D <sup>1</sup>H–<sup>1</sup>H NMR TOCSY spectra that are indicative of the binding of **11** to HSA at the Cys<sup>34</sup> residue (Figure 3). Specifically, the Cys<sup>34</sup> residue of HSA (left panel) is partially disulfide bonded to endogenous NPSH, resulting in the splitting of the Hε1 resonance of the His<sup>3</sup> residue at ~8.2 ppm (left panel expanded inset box). Chemical reduction of HSA to mHSA (Cys<sup>34</sup> in thiol/thiolate form) results in disappearance of the splitting of this resonance (center panel expanded inset box). Incubation of **11** with mHSA (1:1) restores the split resonance (right panel expanded inset box), indicating that disulfide bond formation has occurred between **11** and the Cys<sup>34</sup> residue.

Additionally, incubation of **11** with HSA results in the appearance of new AMX systems at ~4.2 ppm, which are consistent with the αH–βH<sub>2</sub> resonances of free cystine (Figure 4, center panel, solid lines) and the slightly more upfield

Scheme 1. Synthesis of Gd-DOTA-monoamide Complexes 3a–e



Scheme 2. Synthesis of Eu-DOTA-monoamide Complex 11

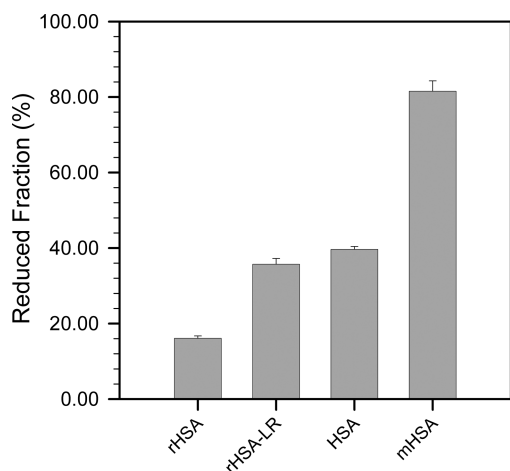
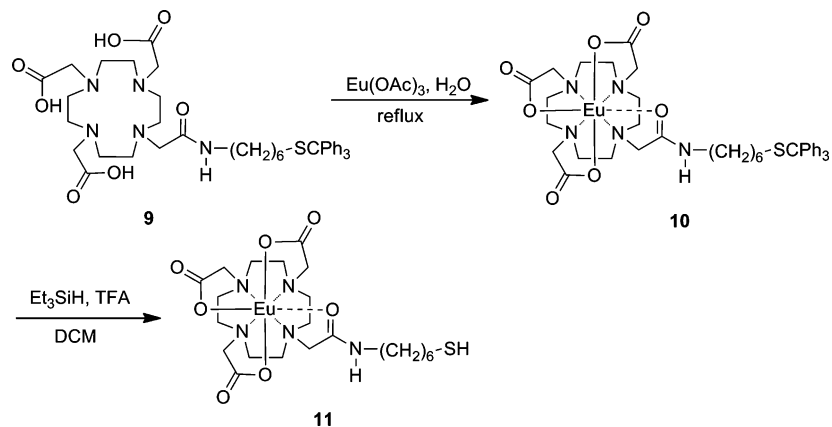


**Figure 1.** Ellman's assay of the thiol content of four types of human serum albumin: recombinant HSA (rHSA), lipid-reduced recombinant HSA (rHSA-LR), human serum albumin purified from donor plasma (HSA), and mercapt-HSA (mHSA) prepared from commercial HSA by the method of Jacobsen.

crosspeaks due either to free cysteine or a mixed disulfide of free cysteine with **11** (Figure 4, center panel, dashed lines). These new AMX systems are not present in spectra of HSA by itself (Figure 4, left panel) and do not appear in spectra of mHSA incubated with **11** (Figure 4, right panel).

The results in Figure 4 suggest that this batch of HSA purified from donor plasma (Sigma) carries cysteine bound to the Cys<sup>34</sup> residue, and that this cysteine is replaced and released by the competitive binding of **11**, followed by oxidation of the free cysteine to cystine or to the mixed disulfide. Any such small molecule thiol would have been removed during the preparation of mHSA, explaining the absence of these crosspeaks in the right panel. These resonances are invisible in spectra of HSA by itself (left panel), most probably due to broadening arising from attachment to the macromolecule. Upon release into solution, the sharper crosspeaks of the small molecule become visible. Taken together, the NMR results in Figures 3 and 4 provide evidence for the binding of **11** to HSA at the targeted Cys<sup>34</sup> residue.

**Binding and Relaxometry.** The binding of compounds **1**, **2**, and **3a–e** to mHSA prepared from commercially obtained HSA was measured at 37 °C in PBS. The measured  $K_A$  values

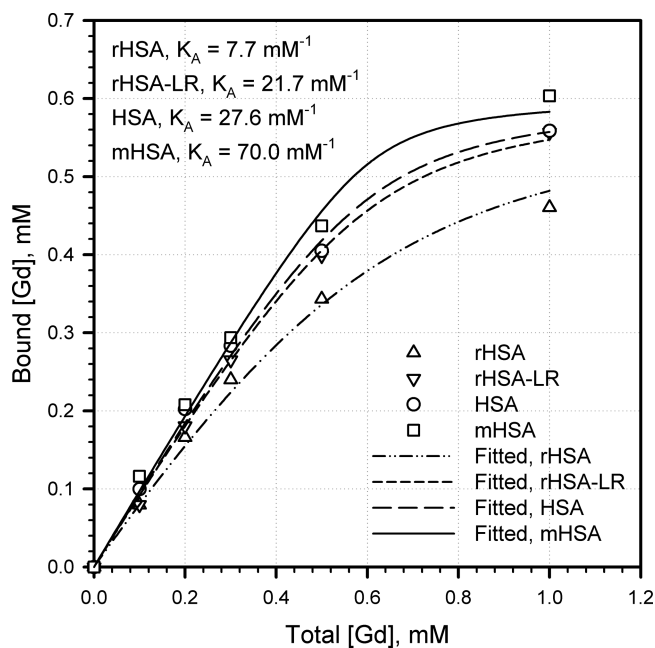


**Figure 2.** Binding of **3c** to rHSA, rHSA-LR, HSA, and mHSA, measured at 37 °C in PBS. Protein concentration was 0.6 mM, and data were fitted to a single-site binding model.

for these compounds showed a steady increase in magnitude with increase in linker length (Table 1). The binding of complexes **1**, **2**, and **3a–3c** to mHSA was well described by a single-site binding model. However, the binding of complexes **3d** and **3e** was not adequately described by a single-site binding model, and for both of these complexes the Gd:mHSA binding stoichiometry exceeded 1:1 at complex concentrations of 1 mM. It is possible that the longer hydrophobic linkers in **3d** and **3e** allow these complexes to bind additionally to lipid-binding sites on HSA.<sup>21</sup> The binding of compounds **1**, **2**, and **3a–3c** to mHSA could be competitively inhibited by addition of homocysteine (Table 1). This supports the hypothesis that disulfide formation between the Gd complex and HSA is an essential component of binding. A decrease in binding with increasing homocysteine concentration was also observed for

complexes **3d** and **3e**, indicating that some fraction of the total binding of these two complexes to mHSA is thiol-sensitive.

The longitudinal water-proton relaxivities ( $r_1$ ) of compounds **1**, **2**, and **3a–3e** were measured at 7 T at 37 °C in PBS in the absence of mHSA to give  $r_{1,\text{free}}$  and in the presence of mHSA to give  $r_{1,\text{bound}}$  (Table 2). As expected,  $r_{1,\text{bound}}$  was observed to be higher than  $r_{1,\text{free}}$  for all complexes, consistent with an increase in molecular reorientation time upon binding of the Gd complex to the macromolecular protein. The increase in  $r_{1,\text{bound}}$  relative to  $r_{1,\text{free}}$  was comparable for all complexes.

## DISCUSSION

There is continuing interest in the development of NMR and MRI biomarkers of tumor redox status. Recently Brindle et al. have detected reduction of hyperpolarized [ $^{13}\text{C}$ ]-dehydroascorbic acid in lymphoma tumors in vivo but no detectable oxidation of [ $^{13}\text{C}$ ]-ascorbic acid in the same tumors, indicating that these tumors maintain a reduced microenvironment.<sup>22</sup> Sherry and co-workers report that a DOTA-tetraamide europium complex with two quinolinium moieties is silent on Chemical Exchange Saturation Transfer (CEST) MRI images in the oxidized form but is activated upon reduction by  $\beta$ -NADH.<sup>23</sup> We have previously demonstrated by dynamic contrast-enhanced MRI that **1** and **2** are retained in vivo longer than the comparably sized Gd-DTPA. The in vivo washout of **1** and **2** is speeded up by an intravenous chase bolus of homocysteine, consistent with the spontaneous binding of these complexes to plasma albumin in a reversible redox-sensitive manner following intravenous administration.<sup>10</sup> Aime and co-workers have reported success in labeling tumor cells in vitro with a Gd-DO3A-based disulfide complex designed to bind to protein thiols on the cell surface.<sup>24</sup> They have also demonstrated uptake into cells in xenograft tumors in vivo after direct injection into the tumor but significantly not following intravenous injection, possibly due to reaction of the disulfide with thiols in plasma and on the surface of blood vessels before it can reach the tumor.<sup>25</sup> We recently utilized **2** to provide a contrast-enhanced MRI biomarker of the response of tumor xenografts to the thiol-modulating drugs buthionine sulfoximine and Imexon.<sup>11</sup> In the present work we have investigated

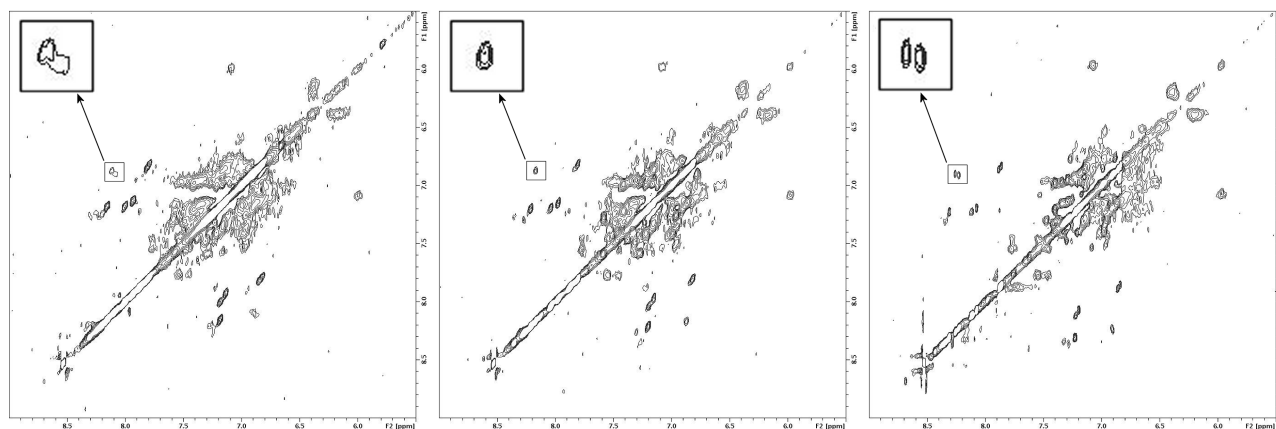


**Figure 3.** Downfield regions of the 2D  $^1\text{H}$ – $^1\text{H}$  NMR TOCSY spectra of human serum albumin in deuterated buffer at pD  $\sim$ 7.4. The Cys<sup>34</sup> residue of HSA (left panel) is partially in a disulfide form, resulting in the splitting of the H $\epsilon$ 1 resonance of the His<sup>3</sup> residue at  $\sim$ 8.2 ppm (expanded inset box). Chemical reduction of HSA to mHSA (Cys<sup>34</sup> in thiol/thiolate form) results in disappearance of the splitting of this resonance (center panel expanded inset box). Incubation of **11** with mHSA (1:1) restores the split resonance (right panel expanded inset box), indicating disulfide bond formation between **11** and the Cys<sup>34</sup> residue.

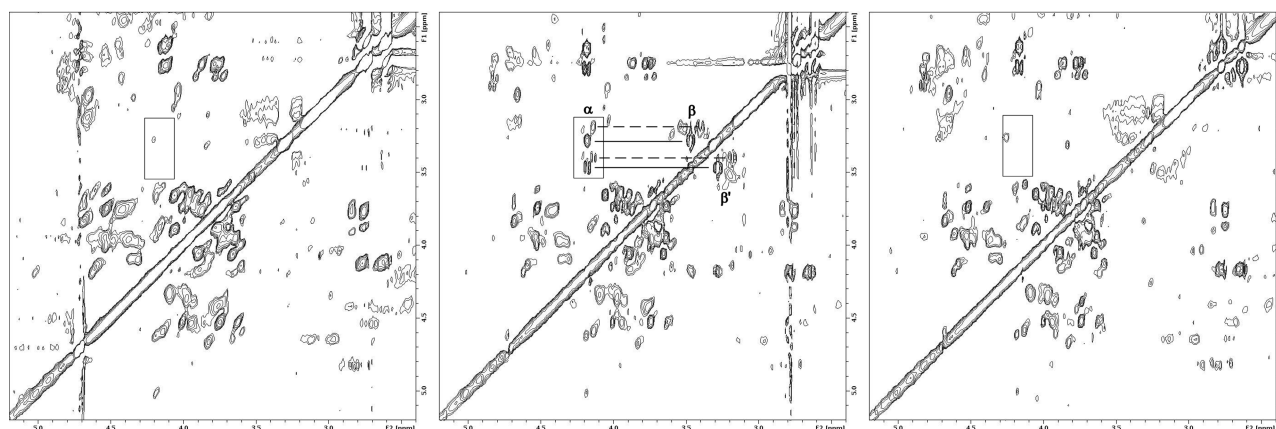


**Figure 4.** Upfield regions of the 2D  $^1\text{H}$ - $^1\text{H}$  NMR TOCSY spectra of human serum albumin in deuterated buffer at pD  $\sim$ 7.4. Incubation of **11** with HSA (1:1) (center panel) results in the appearance of new AMX systems at 3.2–4.2 ppm (inset box) which are consistent with the  $\alpha\text{H}$ - $\beta\text{H}_2$  resonances of free cysteine (solid lines) as well as either free cysteine or the mixed disulfide of free cysteine and **11** (dashed lines). These new crosspeaks are not found in the corresponding region of the spectra of HSA by itself (left panel) or when **11** is incubated with mHSA (1:1) (right panel). This suggests the release of cysteine bound to HSA at Cys $^{34}$  by competitive binding of **11** to that site, followed by oxidation of the free cysteine to cystine or the mixed disulfide.

**Table 1.** Inhibition of Binding of Compounds **1**, **2**, and **3a–3e** to 0.6 mM mHSA<sup>a</sup>

homocysteine concentration (mM)	0.0	0.5	1.0	2.0
compound	$K_A$ (mM $^{-1}$ )			
<b>1</b>	6.0 $\pm$ 1.5	2.8 $\pm$ 1.2	1.2 $\pm$ 0.4	0.7 $\pm$ 0.2
<b>3a</b>	11.3 $\pm$ 1.5	5.1 $\pm$ 1.5	1.4 $\pm$ 0.4	0.4 $\pm$ 0.4
<b>3b</b>	16.8 $\pm$ 8.3	11.7 $\pm$ 5.0	6.9 $\pm$ 2.4	4.4 $\pm$ 2.1
<b>2</b>	32.1 $\pm$ 17.9	14.7 $\pm$ 3.3	8.5 $\pm$ 3.0	4.8 $\pm$ 1.3
<b>3c</b>	69.8 $\pm$ 7.2	32.9 $\pm$ 3.5	15.8 $\pm$ 3.3	6.6 $\pm$ 1.4
<b>3d</b>	83.4 $\pm$ 17.0 <sup>b</sup>	42.6 $\pm$ 23.9 <sup>b</sup>	26.0 $\pm$ 14.5 <sup>b</sup>	12.8 $\pm$ 7.2 <sup>b</sup>
<b>3e</b>				

<sup>a</sup>Measured at 37  $^\circ\text{C}$ . <sup>b</sup>Poor fit to a single-site binding equation, and the Gd:HSA binding stoichiometry exceeds 1:1 at 1 mM [Gd], but binding decreased as the concentration of homocysteine was increased.

**Table 2.** Longitudinal MRI Relaxivities of Compounds **1**, **2**, and **3a–3e** in PBS ( $r_{1,\text{free}}$ ) and when Bound to mHSA ( $r_{1,\text{bound}}$ )<sup>a</sup>

compound	$r_{1,\text{free}}$ (1/mM s)	$r_{1,\text{bound}}$ (1/mM s)
<b>1</b>	3.48 $\pm$ 0.15	4.62 $\pm$ 0.14
<b>3a</b>	3.01 $\pm$ 0.11	4.60 $\pm$ 0.55
<b>3b</b>	3.13 $\pm$ 0.04	4.64 $\pm$ 0.31
<b>2</b>	3.24 $\pm$ 0.09	4.78 $\pm$ 0.19
<b>3c</b>	3.75 $\pm$ 0.21	5.68 $\pm$ 0.57
<b>3d</b>	3.31 $\pm$ 0.12	5.85 $\pm$ 0.34
<b>3e</b>	3.00 $\pm$ 0.15	4.73 $\pm$ 0.19

<sup>a</sup>Measured at 37  $^\circ\text{C}$  and 7 T.

the influence of alkyl linker length on the HSA binding properties of the set of C3–C9 homologues, including **1** and **2**.

The binding of complexes **1**, **2**, and **3a–3c** to HSA was well-described by single-site binding equations, while the  $K_A$  values for complexes **3d** and **3e** with C-8 and C-9 linkers, respectively, were higher than predicted and indicative of multisite binding. The binding of all complexes to HSA was inhibited by homocysteine, suggesting that covalent attachment by formation of a disulfide link with Cys $^{34}$  is an important component of binding.

The measured  $K_A$  for binding of **3c** to four different HSA preparations was not identical, and this could be explained by differences in the Cys $^{34}$  thiol oxidation states of the

preparations. 2D  $^1\text{H}$ - $^1\text{H}$  NMR TOCSY provided evidence for the covalent binding of **11**, the europium-bearing analog of **2**, to Cys $^{34}$  of mHSA. This is taken as evidence for similar binding behaviors for **1**, **2**, and **3a–3e** with respect to covalent attachment to Cys $^{34}$ .

Finally, the longitudinal MRI relaxivities of complexes **1**, **2**, and **3a–3e** are higher when bound to HSA than when free. The relaxivity of a gadolinium agent depends on a number of factors: the applied field ( $B_0$ ), the electronic relaxation time ( $T_{1e}$ ), the correlation time for rotational motion ( $\tau_R$ ), the inner-sphere hydration number ( $q$ ), the rate of water (or water-proton) exchange at the metal ion (i.e.,  $k_{\text{ex}} = 1/\tau_m$  for the inner-sphere), the distance between the Gd(III) ion and the water-proton ( $r_{\text{Gd-H}}$ ), and corresponding parameters for second-sphere and outer-sphere relaxation.<sup>26,27</sup> The observed higher values of  $r_{1,\text{bound}}$  of our complexes relative to the corresponding values of  $r_{1,\text{free}}$  are consistent with a slowing down of the  $\tau_R$  of the Gd–H axis upon binding to the macromolecule.

## CONCLUSIONS

The difference between  $r_{1,\text{bound}}$  and  $r_{1,\text{free}}$  of DOTA-monoamide thiol complexes of gadolinium can be exploited to produce enhancement in MRI images that is dependent on the local redox status. We have recently demonstrated that the shortening of MRI longitudinal relaxation times ( $T_1$ ) of xenograft tumors after injection of **2** was greater in mice that were treated with the thiol-oxidizing drug Imexon relative to

saline treatment.<sup>11</sup> High tumor levels of thiols can decrease tumor sensitivity to certain drugs and to radiotherapy. An MRI method for post-therapy assessment of tumor response to redox-modulating therapies would assist in the development of novel redox-modulating drugs for preadministration or coadministration with chemotherapy or radiotherapy. The results reported here indicate that **3c** would perform better than **2** as an MRI biomarker of tumor response to redox-active therapies due to its superior thiol-sensitive binding affinity for HSA. To improve upon **2** and **3c**, we are pursuing strategies to increase  $r_{1,\text{bound}}$  by speeding up  $\tau_m$  at the HSA-bound gadolinium. We are also exploring strategies to quench  $r_{1,\text{bound}}$  by increasing  $r_{\text{Gd-H}}$  when the complex is bound to HSA, with a view to creating an MRI contrast agent that will highlight only highly reducing tissue microenvironments.

## EXPERIMENTAL SECTION

**Synthesis.** Reactions were conducted with flame-dried glassware under a positive pressure of argon. Hydroscopic solvents were transferred via an oven-dried syringe or cannula. All reagents and solvents were commercially available and were used as received. Solutions were concentrated *in vacuo* using a rotary evaporator. Analytical thin-layer chromatography (TLC) was performed on precoated silica gel 60 F-254 glass plates. TLC visualization required using UV light and/or staining. Anisaldehyde stain (100 mL anisaldehyde, 50 mL glacial AcOH, 100 mL conc H<sub>2</sub>SO<sub>4</sub>, 1 L 95% EtOH) and PMA stain (5 g phosphomolybdic acid, 100 mL 95% EtOH) were the most commonly used TLC stains. Flash and gravity chromatography were performed using silica gel 60 (230–400 mesh). Melting points are uncorrected. Nuclear magnetic resonance (NMR) experiments were performed on a 500 MHz spectrometer. NMR spectra were referenced to TMS (0.00 ppm), CDCl<sub>3</sub> (7.24 ppm, 77.0 ppm), CD<sub>3</sub>OD (3.31 ppm), or CH<sub>3</sub>CN in D<sub>2</sub>O (119.68). Mass spectrometry was conducted using ESI. Free gadolinium content in the final compounds was analyzed by means of the xylenol orange test<sup>28</sup> and found to be negative. Purities of the final compounds were >95% and were determined by RP-HPLC analysis (see the Supporting Information).

**Procedure for Synthesis of Tritylthioalkylphthalimides 5a–5e: 2-(7-(Tritylthio)heptyl)isoindoline-1,3-dione (5c).** To a suspension of NaH (0.59 g, 24.7 mmol) in dry DMF (25 mL) at 0 °C under argon was added triphenylmethanethiol (6.8 g, 24.7 mmol) portionwise with cooling and under an argon atmosphere. After 0.5 h, a solution of bromide **4c** (8.0 g, 24.7 mmol) in DMF (25 mL) was added dropwise with stirring. The reaction mixture was stirred for another 5 min, brought to rt, and was stirred overnight. Ethyl acetate (200 mL) was added to the reaction mixture and the organic phase was washed with water (3 × 100 mL), brine (50 mL), dried (MgSO<sub>4</sub>), and filtered. Concentration under reduced pressure gave **5c** (10.0 g, 19.3 mmol, 83%) as a white solid, mp 72–73 °C, *R*<sub>f</sub> 0.62 (EtOAc/hexanes 3:7). <sup>1</sup>H NMR (500 MHz, CDCl<sub>3</sub>) δ 1.15–1.28 (8, m), 1.36 (2, m), 1.61 (2, quintet, *J* = 7.5 Hz), 2.11 (2, t, *J* = 7.5 Hz), 3.63 (2, t, *J* = 7.5 Hz), 7.17–7.21 (3, m), 7.24–7.28 (6, m), 7.38–7.41 (6, m), 7.69 (2, dd, *J* = 5.4 Hz, 3.0 Hz), 7.83 (2, dd, *J* = 5.4 Hz, 3.0 Hz); <sup>13</sup>C NMR (125 MHz, CDCl<sub>3</sub>) δ 26.6, 28.4, 28.5, 28.7, 28.8, 31.9, 37.7, 40.2, 66.3, 123.1, 126.4, 127.7, 129.5, 132.1, 133.7, 145.0, 168.3; HRMS (ESI<sup>+</sup>, *m/z*) calculated for C<sub>34</sub>H<sub>33</sub>NNaO<sub>2</sub>S 542.2124, found 542.2129 (M + Na)<sup>+</sup>.

**2-(4-(Tritylthio)butyl)isoindoline-1,3-dione (5a).** Yield 93%, white solid, mp 126–127 °C, *R*<sub>f</sub> 0.55 (EtOAc/hexanes 3:7). <sup>1</sup>H NMR (500 MHz, CDCl<sub>3</sub>) δ 1.40 (2, quintet, *J* = 7.0 Hz), 1.62 (2, quintet, *J* = 7.0 Hz), 2.17 (2, t, *J* = 7.0 Hz), 3.55 (2, t, *J* = 7.0 Hz), 7.00–7.18 (3, m), 7.22–7.27 (6, m), 7.35–7.42 (6, m), 7.65–7.72 (2, dd, *J* = 5.5 Hz, 3 Hz), 7.79–7.83 (2, dd, *J* = 5.5 Hz, 3 Hz); <sup>13</sup>C NMR (125 MHz, CDCl<sub>3</sub>) δ 25.9, 28.0, 31.4, 37.5, 66.4, 123.1, 126.4, 127.7, 129.3, 129.5, 132.0, 133.8, 144.8, 168.1; HRMS (ESI<sup>+</sup>, *m/z*) calculated for C<sub>31</sub>H<sub>27</sub>NNaO<sub>2</sub>S 500.1655, found 500.1648 (M + Na)<sup>+</sup>.

**2-(5-(Tritylthio)pentyl)isoindoline-1,3-dione (5b).** Yield 81%, white solid, mp 124–125 °C, *R*<sub>f</sub> 0.57 (EtOAc/hexanes 3:7). <sup>1</sup>H NMR (500 MHz, CDCl<sub>3</sub>) δ 1.28 (2, quintet, *J* = 7.0 Hz), 1.41 (2, quintet, *J* = 7.0 Hz), 1.54 (2, quintet, *J* = 7.0 Hz), 2.13 (2, t, *J* = 7.0 Hz), 3.59 (2, t, *J* = 7.0 Hz), 7.15–7.20 (3, m), 7.22–7.28 (6, m), 7.35–7.40 (6, m), 7.68–7.70 (2, dd, *J* = 5.0 Hz, 3 Hz), 7.81–7.83 (2, dd, *J* = 5.5 Hz, 3 Hz); <sup>13</sup>C NMR (125 MHz, CDCl<sub>3</sub>) δ 26.3, 28.2, 28.3, 31.7, 37.8, 66.4, 123.1, 126.4, 127.7, 129.5, 132.1, 133.8, 144.9, 168.2; HRMS (ESI<sup>+</sup>, *m/z*) calculated for C<sub>32</sub>H<sub>29</sub>NNaO<sub>2</sub>S 514.1811, found 514.1807 (M + Na)<sup>+</sup>.

**2-(8-(Tritylthio)octyl)isoindoline-1,3-dione (5d).** Yield 91%, tan solid, mp 68–71 °C, *R*<sub>f</sub> 0.58 (EtOAc/hexanes 3:7). <sup>1</sup>H NMR (500 MHz, CDCl<sub>3</sub>) δ 1.20–1.28 (8, m), 1.32–1.38 (2, m), 1.60–1.65 (2, m), 2.11 (2, t, *J* = 7.0 Hz), 3.65 (2, t, *J* = 7.0 Hz), 7.17–7.21 (3, m), 7.24–7.28 (6, m), 7.37–7.41 (6, m), 7.68–7.71 (2, m), 7.81–7.84 (2, m); <sup>13</sup>C NMR (125 MHz, CDCl<sub>3</sub>) δ 26.7, 28.5, 28.8, 28.9, 31.9, 38.0, 66.3, 123.0, 126.3, 127.6, 129.5, 132.1, 133.7, 145.0, 168.2; HRMS (ESI<sup>+</sup>, *m/z*) calculated for C<sub>35</sub>H<sub>35</sub>NNaO<sub>2</sub>S 556.2281, found 556.2275 (M + Na)<sup>+</sup>.

**2-(9-(Tritylthio)nonyl)isoindoline-1,3-dione (5e).** Yield 89%, white solid, mp 59–61 °C, *R*<sub>f</sub> 0.56 (EtOAc/hexanes 3:7). <sup>1</sup>H NMR (500 MHz, CDCl<sub>3</sub>) δ 1.10–1.38 (12, m), 1.64 (2, m), 2.11 (2, t, *J* = 7.0 Hz), 3.65 (2, t, *J* = 7.0 Hz), 7.18–7.21 (3, m), 7.25–7.30 (6, m), 7.39–7.43 (6, m), 7.69 (2, m), 7.83 (2, m); <sup>13</sup>C NMR (125 MHz, CDCl<sub>3</sub>) δ 26.8, 28.5, 28.9, 29.0, 29.2, 31.9, 38.0, 66.3, 123.1, 126.4, 127.7, 127.8, 129.5, 133.7, 145.0, 168.4; HRMS (ESI<sup>+</sup>, *m/z*) calculated for C<sub>36</sub>H<sub>37</sub>NNaO<sub>2</sub>S 570.2429, found 570.2437 (M + Na)<sup>+</sup>.

**Procedure for Synthesis of Tritylthioalkylamines 6a–6e: 7-(Tritylthio)heptan-1-amine (6c).** To a suspension of **5c** (6.0 g, 11.5 mmol) in absolute ethanol (75 mL) was added hydrazine hydrate (1.84 g, 57.8 mmol, 1.8 mL) and the mixture was heated to reflux. After 5 h, the mixture was filtered and the filtrate concentrated under reduced pressure. CHCl<sub>3</sub> (100 mL) was added to the residue, the mixture stirred for 0.5 h, and filtered. The precipitate was washed with CHCl<sub>3</sub> (100 mL) and the combined organic fractions were washed with water (3 × 100 mL), dried (MgSO<sub>4</sub>), filtered, and concentrated. The crude was purified by flash chromatography on silica gel eluted with CH<sub>2</sub>Cl<sub>2</sub>/MeOH/aq NH<sub>4</sub>OH (5:3:0.1) to afford **6c** (3.6 g, 9.2 mmol, 80%) as a white solid, mp 74–76 °C, *R*<sub>f</sub> 0.36 (CH<sub>2</sub>Cl<sub>2</sub>/MeOH/aq NH<sub>4</sub>OH 5:3:0.1). <sup>1</sup>H NMR (500 MHz, CDCl<sub>3</sub>) δ 1.13–1.27 (6, m), 1.37 (4, m), 2.12 (2, t, *J* = 7.5 Hz), 2.63 (2, t, *J* = 7.0 Hz), 7.17–7.20 (3, m), 7.25–7.28 (6, m), 7.40 (6, m); <sup>13</sup>C NMR (125 MHz, CDCl<sub>3</sub>) δ 26.6, 28.5, 28.9, 29.0, 31.9, 33.7, 42.2, 66.3, 126.4, 127.7, 129.5, 145.0; HRMS (ESI<sup>+</sup>, *m/z*) calculated for C<sub>26</sub>H<sub>32</sub>NS 390.2250, found 390.2249 (M + H)<sup>+</sup>.

**4-(Tritylthio)butan-1-amine (6a).** Yield 86%, white solid, mp 88–92 °C, *R*<sub>f</sub> 0.46 (CH<sub>2</sub>Cl<sub>2</sub>/MeOH/aq NH<sub>4</sub>OH 5:3:0.1). <sup>1</sup>H NMR (500 MHz, CDCl<sub>3</sub>) δ 1.20–1.48 (4, m), 2.16 (2, t, *J* = 7.0 Hz), 2.53 (2, t, *J* = 7.0 Hz), 7.17–7.21 (3, m), 7.24–7.28 (6, m), 7.38–7.43 (6, m); <sup>13</sup>C NMR (125 MHz, CDCl<sub>3</sub>) δ 31.6, 32.8, 41.4, 66.2, 126.3, 127.6, 129.3, 144.7; HRMS (ESI<sup>+</sup>, *m/z*) calculated for C<sub>23</sub>H<sub>25</sub>NNaS 370.1600, found 370.1604 (M + Na)<sup>+</sup>.

**5-(Tritylthio)pentan-1-amine (6b).** Yield 86%, white solid, mp 85–89 °C, *R*<sub>f</sub> 0.32 (CH<sub>2</sub>Cl<sub>2</sub>/MeOH/aq NH<sub>4</sub>OH 5:3:0.1); <sup>1</sup>H NMR (500 MHz, CDCl<sub>3</sub>) δ 1.21–1.32 (2, m), 1.35–1.48 (4, m), 2.15 (2, t, *J* = 7.0 Hz), 2.58 (2, t, *J* = 7.0 Hz), 7.16–7.21 (3, m), 7.24–7.28 (6, m), 7.38–7.42 (6, m); <sup>13</sup>C NMR (125 MHz, CDCl<sub>3</sub>) δ 26.3, 28.4, 31.9, 33.2, 41.9, 66.4, 126.4, 127.7, 129.5, 144.9; HRMS (ESI<sup>+</sup>, *m/z*) calculated for C<sub>24</sub>H<sub>27</sub>NNaS 384.1762, found 384.1760 (M + Na)<sup>+</sup>.

**8-(Tritylthio)octan-1-amine (6d).** Yield 92%, light yellow solid, mp 45–46 °C, *R*<sub>f</sub> 0.33 (CH<sub>2</sub>Cl<sub>2</sub>/MeOH/aq NH<sub>4</sub>OH 5:3:0.1). <sup>1</sup>H NMR (500 MHz, CDCl<sub>3</sub>) δ 1.10–1.30 (10, m), 1.34–1.44 (2, m), 2.13 (2, t, *J* = 7.0 Hz), 2.65 (2, t, *J* = 7.0 Hz), 7.17–7.22 (3, m), 7.24–7.29 (6, m), 7.38–7.43 (6, m); <sup>13</sup>C NMR (125 MHz, CDCl<sub>3</sub>) δ 28.6, 28.9, 29.1, 29.2, 32.0, 33.6, 42.2, 66.3, 126.4, 127.7, 129.5, 145.0; HRMS (ESI<sup>+</sup>, *m/z*) calculated for C<sub>27</sub>H<sub>34</sub>NS 404.2406, found 404.2406 (M + H)<sup>+</sup>.

**9-(Tritylthio)nonan-1-amine (6e).** Yield 81%, viscous oil, *R*<sub>f</sub> 0.29 (CH<sub>2</sub>Cl<sub>2</sub>/MeOH/aq NH<sub>4</sub>OH 5:3:0.1). <sup>1</sup>H NMR (500 MHz, CDCl<sub>3</sub>) δ 1.10–1.30 (10, m), 1.35–1.45 (4, m), 2.12 (2, t, *J* = 7.5 Hz), 2.66 (2,

$t, J = 7.0$  Hz), 7.17–7.22 (3, m), 7.24–7.29 (6, m), 7.38–7.43 (6, m);  $^{13}\text{C}$  NMR (125 MHz,  $\text{CDCl}_3$ )  $\delta$  28.8, 28.5, 29.9, 29.1, 29.3, 32.0, 33.7, 42.2, 66.3, 126.4, 127.7, 129.5, 145.0; HRMS ( $\text{ESI}^+$ ,  $m/z$ ) calculated for  $\text{C}_{28}\text{H}_{36}\text{N}_5$  418.2563, found 418.2557 ( $\text{M} + \text{H}$ ) $^+$ .

**Procedure for the Synthesis of DOTA-based Tricarboxylic Acids 7a–7e:** [1,4,7-Tris(carboxymethyl)-10-[N-(7-tritylthioheptyl)carbamoyl]-1,4,7,10-tetraazacyclododecane (7c). 1,4,7,10-Tetraazacyclododecane-1,4,7,10-tetraacetic acid (DOTA, 2.62 g, 6.0 mmol) was dissolved in water (3 mL), lyophilized, and dissolved in DMF/TEA (4:1, v/v, 150 mL) and stirred at rt for 24 h. Isobutyl chloroformate (0.41 g, 3 mmol, 0.39 mL) was then added to the reaction mixture at 0 °C. After 1 h, amine 6c (0.78 g, 2.0 mmol) was added and the reaction mixture stirred. After 48 h, the solvent was removed under reduced pressure and the crude solid was loaded onto a gravity silica gel column. Elution with  $\text{CH}_2\text{Cl}_2/\text{MeOH}/\text{aq NH}_4\text{OH}$  (5:3:0.3) followed by removal of solvents gave a viscous oil which was dissolved in a minimal amount of water and freeze-dried to afford 7c (1.08 g, 1.39 mmol, 70%), which was obtained as a white fluffy solid, mp 200–202 °C (dec),  $R_f$  0.57 ( $\text{CH}_2\text{Cl}_2/\text{MeOH}/\text{aq NH}_4\text{OH}$  5:3:1).  $^1\text{H}$  NMR (500 MHz,  $\text{CD}_3\text{OD}$ )  $\delta$  1.15–1.28 (6, m), 1.35 (2, quintet,  $J = 7.5$  Hz), 1.45 (2, m), 2.12 (4, m), 2.29 (4, m), 2.85 (8, m), 3.12 (8, m), 3.5–3.8 (4, m), 7.18–7.23 (3, m), 7.24–7.29 (6, m), 7.36–7.39 (6, m);  $^{13}\text{C}$  NMR (125 MHz,  $\text{D}_2\text{O}$ )  $\delta$  27.0, 29.3, 32.4, 40.1, 48.5, 59.5, 61.6, 66.8, 127.1, 128.4, 129.0, 145.4, 174.0, 180.2; HRMS ( $\text{ESI}^+$ ,  $m/z$ ) calculated for  $\text{C}_{42}\text{H}_{58}\text{N}_5\text{O}_7\text{S}$  776.4051, found 776.4052 ( $\text{M} + \text{H}$ ) $^+$ .

[1,4,7-Tris(carboxymethyl)-10-[N-(4-tritylthiobutyl)carbamoyl]-1,4,7,10-tetraazacyclododecane (7a). Yield 74%, white fluffy solid, 210–214 °C (dec),  $R_f$  0.56 ( $\text{CH}_2\text{Cl}_2/\text{MeOH}/\text{aq NH}_4\text{OH}$  5:3:1).  $^1\text{H}$  NMR (500 MHz,  $\text{CD}_3\text{OD}$ )  $\delta$  1.35 (2, quintet,  $J = 7.5$  Hz), 1.43 (2, m), 2.17 (4, t,  $J = 7.0$  Hz), 2.28 (4, m), 2.84 (8, m), 3.2 (8, m), 3.50–3.75 (4, m), 7.19–7.23 (3, m), 7.26–7.30 (6, m), 7.36–7.39 (6, m);  $^{13}\text{C}$  NMR (125 MHz,  $\text{D}_2\text{O}$ )  $\delta$  26.4, 28.5, 39.8, 48.8, 59.3, 61.5, 66.9, 127.2, 128.4, 129.9, 145.3, 174.1, 180.3. HRMS ( $\text{ESI}^+$ ,  $m/z$ ) calculated for  $\text{C}_{39}\text{H}_{52}\text{N}_5\text{O}_7\text{S}$  734.3582, found 734.3586 ( $\text{M} + \text{H}$ ) $^+$ .

[1,4,7-Tris(carboxymethyl)-10-[N-(5-tritylthiopentyl)carbamoyl]-1,4,7,10-tetraazacyclododecane (7b). Yield 74%, white fluffy solid, 204–208 °C (dec),  $R_f$  0.54 ( $\text{CH}_2\text{Cl}_2/\text{MeOH}/\text{aq NH}_4\text{OH}$  5:3:1).  $^1\text{H}$  NMR (500 MHz,  $\text{CD}_3\text{OD}$ )  $\delta$  1.26 (2, m), 1.33–1.42 (4, m), 2.16 (4, m), 2.28 (4, m), 2.85 (8, m), 3.26 (8, m), 3.50–3.75 (4, m), 7.19–7.23 (3, m), 7.26–7.30 (6, m), 7.36–7.39 (6, m);  $^{13}\text{C}$  NMR (125 MHz,  $\text{D}_2\text{O}$ )  $\delta$  26.38, 28.6, 32.4, 39.7, 48.4, 57.5, 59.4, 66.7, 127.1, 128.3, 129.8, 145.3, 173.9, 180.1; HRMS ( $\text{ESI}^+$ ,  $m/z$ ) calculated for  $\text{C}_{40}\text{H}_{54}\text{N}_5\text{O}_7\text{S}$  748.3738, found 748.3743 ( $\text{M} + \text{H}$ ) $^+$ .

[1,4,7-Tris(carboxymethyl)-10-[N-(8-tritylthiooctyl)carbamoyl]-1,4,7,10-tetraazacyclododecane (7d). Yield 75%, white fluffy solid, 174 °C (dec),  $R_f$  0.5 ( $\text{CH}_2\text{Cl}_2/\text{MeOH}/\text{aq NH}_4\text{OH}$  5:3:0.5).  $^1\text{H}$  NMR (500 MHz,  $\text{CD}_3\text{OD}$ )  $\delta$  1.14–1.28 (10, m), 1.34 (2, m), 1.47 (2, m), 2.12 (2, m), 2.31 (4, m), 2.85 (8, m), 3.10–3.16 (8, m), 3.50–3.80 (4, m), 7.18–7.31 (9, m), 7.36–7.41 (6, m);  $^{13}\text{C}$  NMR (125 MHz,  $\text{D}_2\text{O}$ )  $\delta$  23.6, 27.3, 28.9, 29.4, 32.3, 39.6, 48.4, 48.7, 51.7, 52.3, 54.7, 56.1, 57.3, 61.7, 66.7, 127.0, 128.3, 129.8, 145.3, 170.2, 171.0, 177.8; HRMS ( $\text{ESI}^+$ ,  $m/z$ ) calculated for  $\text{C}_{43}\text{H}_{60}\text{N}_5\text{O}_7\text{S}$  790.4208, found 790.4195 ( $\text{M} + \text{H}$ ) $^+$ .

[1,4,7-Tris(carboxymethyl)-10-[N-(9-tritylthiononyl)carbamoyl]-1,4,7,10-tetraazacyclododecane (7e). Yield 72%, white fluffy solid, 176–180 °C (dec),  $R_f$  0.51 ( $\text{CH}_2\text{Cl}_2/\text{MeOH}/\text{aq NH}_4\text{OH}$  5:3:0.5).  $^1\text{H}$  NMR (500 MHz,  $\text{CD}_3\text{OD}$ )  $\delta$  1.12–1.37 (14, m), 1.49 (2, m), 2.11 (2, t,  $J = 7.5$  Hz), 3.00 (8, m), 3.17 (3, m), 3.25–3.50 (9, m), 3.66 (4, m), 7.28–7.21 (3, m), 7.24–7.28 (6, m), 7.37–7.40 (6, m);  $^{13}\text{C}$  NMR (125 MHz,  $\text{D}_2\text{O}$ )  $\delta$  27.4, 29.0, 29.5, 29.8, 32.4, 39.7, 48.8, 51.8, 52.3, 57.4, 66.8, 127.1, 128.3, 129.8, 145.4, 170.2, 171.0, 178.0; HRMS ( $\text{ESI}^+$ ,  $m/z$ ) calculated for  $\text{C}_{44}\text{H}_{62}\text{N}_5\text{O}_7\text{S}$  804.4364, found 804.4364 ( $\text{M} + \text{H}$ ) $^+$ .

**Procedure for Synthesis of Gadolinium Complexes 8a–8e:** [1,4,7-Tris(carboxymethyl)-10-[N-(7-tritylthioheptyl)carbamoyl]-1,4,7,10-tetraazacyclododecanato}gadolinium (8c). To a solution of 7c (0.75 g, 0.96 mmol) in water (10 mL) was added  $\text{Gd}(\text{OAc})_3$  (0.32 g, 0.96 mmol) and the mixture was heated to reflux. After 2 h, the reaction mixture was cooled, the solvent

concentrated in vacuo, and the residue loaded onto a flash silica gel column. Elution with  $\text{CH}_2\text{Cl}_2/\text{MeOH}/\text{aq NH}_4\text{OH}$  (5:3:0.5) followed by removal of solvents gave a viscous oil which was dissolved in a minimum amount of water and freeze-dried. By this procedure 8c (0.80 g, 0.86 mmol, 94%) was obtained as a white fluffy solid, 256–260 °C (dec),  $R_f$  0.54 ( $\text{CH}_2\text{Cl}_2/\text{MeOH}/\text{aq NH}_4\text{OH}$  5:3:1). HRMS ( $\text{ESI}^+$ ,  $m/z$ ) calculated for  $\text{C}_{42}\text{H}_{55}\text{GdN}_5\text{O}_7\text{S}$  931.3066, found 931.3067 ( $\text{M} + \text{H}$ ) $^+$ .

[1,4,7-Tris(carboxymethyl)-10-[N-(4-tritylthiobutyl)carbamoyl]-1,4,7,10-tetraazacyclododecanato}gadolinium (8a). Yield 85%, a white fluffy solid, 264–268 °C (dec),  $R_f$  0.55 ( $\text{CH}_2\text{Cl}_2/\text{MeOH}/\text{aq NH}_4\text{OH}$  5:3:1). HRMS ( $\text{ESI}^+$ ,  $m/z$ ) calculated for  $\text{C}_{39}\text{H}_{49}\text{GdN}_5\text{O}_7\text{S}$  889.2588, found 889.2581 ( $\text{M} + \text{H}$ ) $^+$ .

[1,4,7-Tris(carboxymethyl)-10-[N-(5-tritylthiopentyl)carbamoyl]-1,4,7,10-tetraazacyclododecanato}gadolinium (8b). Yield 91%, a white fluffy solid, 247–250 °C (dec),  $R_f$  0.54 ( $\text{CH}_2\text{Cl}_2/\text{MeOH}/\text{aq NH}_4\text{OH}$  5:3:1). HRMS ( $\text{ESI}^+$ ,  $m/z$ ) calculated for  $\text{C}_{40}\text{H}_{51}\text{GdN}_5\text{O}_7\text{S}$  903.2752, found 903.2740.

[1,4,7-Tris(carboxymethyl)-10-[N-(8-tritylthiooctyl)carbamoyl]-1,4,7,10-tetraazacyclododecanato}gadolinium (8d). Yield 89%, a white fluffy solid, 230–234 °C (dec),  $R_f$  0.53 ( $\text{CH}_2\text{Cl}_2/\text{MeOH}/\text{aq NH}_4\text{OH}$  5:3:1). HRMS ( $\text{ESI}^+$ ,  $m/z$ ) calculated for  $\text{C}_{43}\text{H}_{57}\text{GdN}_5\text{O}_7\text{S}$  945.3214, found 942.3217 ( $\text{M} + \text{H}$ ) $^+$ .

[1,4,7-Tris(carboxymethyl)-10-[N-(9-tritylthiononyl)carbamoyl]-1,4,7,10-tetraazacyclododecanato}gadolinium (8e). Yield 89%, a white fluffy solid, 218 °C (dec),  $R_f$  0.53 ( $\text{CH}_2\text{Cl}_2/\text{MeOH}/\text{aq NH}_4\text{OH}$  5:3:1). HRMS ( $\text{ESI}^+$ ,  $m/z$ ) calculated for  $\text{C}_{44}\text{H}_{59}\text{GdN}_5\text{O}_7\text{S}$  959.3379, found 959.3396 ( $\text{M} + \text{H}$ ) $^+$ .

**Procedure for Synthesis of Gadolinium Complexes 3a–3e:** [1,4,7-Tris(carboxymethyl)-10-[N-(7-mercaptoheptyl)carbamoyl]-1,4,7,10-tetraazacyclododecanato}gadolinium (3c). To a solution of 8c (0.82 g, 0.88 mmol) and  $\text{Et}_3\text{SiH}$  (0.12 g, 1.01 mmol, 0.16 mL) in  $\text{CH}_2\text{Cl}_2$  (30 mL) was added TFA (1.2 mL, 4% v/v) and the mixture was stirred at room temperature. After 10 min, volatiles were removed in vacuo, the residue was dissolved in  $\text{EtOAc}$  (20 mL), and the solution was extracted with water ( $2 \times 10$  mL). The organic layer was discarded and the aqueous layers were lyophilized. Flash chromatography of the residue on reverse phase silica gel ( $\text{H}_2\text{O}/\text{CH}_3\text{CN}$  6:4), followed by lyophilization, gave 0.55 g (0.80 mmol, 91%) of the free thiol 3c as a white fluffy solid, 310 °C (dec),  $R_f$  0.51 ( $\text{H}_2\text{O}/\text{CH}_3\text{CN}$  6:4). HRMS ( $\text{ESI}^+$ ,  $m/z$ ) calculated for  $\text{C}_{23}\text{H}_{41}\text{GdN}_5\text{O}_7\text{S}$  689.1965, found 689.1956 ( $\text{M} + \text{H}$ ) $^+$ .

[1,4,7-Tris(carboxymethyl)-10-[N-(4-mercaptobutyl)carbamoyl]-1,4,7,10-tetraazacyclododecanato}gadolinium (3a). Yield 82%, a white fluffy solid, 230 °C (dec),  $R_f$  0.68 ( $\text{H}_2\text{O}/\text{CH}_3\text{CN}$  6:4). HRMS ( $\text{ESI}^+$ ,  $m/z$ ) calculated for  $\text{C}_{21}\text{H}_{35}\text{GdN}_5\text{O}_7\text{S}$  647.1495, found 647.1491 ( $\text{M} + \text{H}$ ) $^+$ .

[1,4,7-Tris(carboxymethyl)-10-[N-(5-mercaptopentyl)carbamoyl]-1,4,7,10-tetraazacyclododecanato}gadolinium (3b). Yield 78%, a white fluffy solid, 200 °C (dec),  $R_f$  0.63 ( $\text{H}_2\text{O}/\text{CH}_3\text{CN}$  6:4). HRMS ( $\text{ESI}^+$ ,  $m/z$ ) calculated for  $\text{C}_{21}\text{H}_{35}\text{GdN}_5\text{O}_7\text{S}$  661.1652, found 661.1644 ( $\text{M} + \text{H}$ ) $^+$ .

[1,4,7-Tris(carboxymethyl)-10-[N-(8-mercaptooctyl)carbamoyl]-1,4,7,10-tetraazacyclododecanato}gadolinium (3d). Yield 65%, a white fluffy solid, 303 °C (dec),  $R_f$  0.42 ( $\text{H}_2\text{O}/\text{CH}_3\text{CN}$  6:4). HRMS ( $\text{ESI}^+$ ,  $m/z$ ) calculated for  $\text{C}_{24}\text{H}_{43}\text{GdN}_5\text{O}_7\text{S}$  703.2122, found 703.2126 ( $\text{M} + \text{H}$ ) $^+$ .

[1,4,7-Tris(carboxymethyl)-10-[N-(8-mercaptooctyl)carbamoyl]-1,4,7,10-tetraazacyclododecanato}gadolinium (3e). Yield 89%, a white fluffy solid, 190 °C (dec),  $R_f$  0.39 ( $\text{H}_2\text{O}/\text{CH}_3\text{CN}$  6:4). HRMS ( $\text{ESI}^+$ ,  $m/z$ ) calculated for  $\text{C}_{25}\text{H}_{45}\text{GdN}_5\text{O}_7\text{S}$  717.2278, found 717.2273 ( $\text{M} + \text{H}$ ) $^+$ .

[1,4,7-Tris(carboxymethyl)-10-[N-(6-tritylthiohexyl)carbamoyl]-1,4,7,10-tetraazacyclododecanato}europium (10). To a solution of 9 $^{10}$  (0.58 g, 0.76 mmol) in water (10 mL) was added  $\text{Eu}(\text{OAc})_3$  (0.25 g, 0.76 mmol) and the mixture heated to reflux. After 2 h, the reaction mixture was cooled, the volatiles were removed in vacuo, and the residue was loaded on a flash silica gel column. Elution with  $\text{CH}_2\text{Cl}_2/\text{MeOH}/\text{aq NH}_4\text{OH}$  (5:3:0.5) followed by removal of solvents gave a viscous oil which was dissolved in a minimum amount of water and freeze-dried. By this procedure, 10 (0.54 g, 0.60 mmol, 79%) was obtained as a white fluffy solid, 254 °C (dec),  $R_f$  0.54

(CH<sub>2</sub>Cl<sub>2</sub>/MeOH/aq NH<sub>4</sub>OH 5:3:1). HRMS (ESI<sup>+</sup>, *m/z*) calculated for C<sub>41</sub>H<sub>53</sub>EuN<sub>3</sub>O<sub>7</sub>S 912.2872, found 912.2863 (M + H)<sup>+</sup>.

**1,4,7-Tris(carboxymethyl)-10-[N-(6-mercaptohexyl)-carbamoyl]-1,4,7,10-tetraazacyclododecanato]europium (11).** To a solution of **10** (0.33 g, 0.36 mmol) and Et<sub>3</sub>SiH (48.0 μg, 0.41 mmol, 65 μL) in CH<sub>2</sub>Cl<sub>2</sub> (15 mL) was added TFA (0.6 mL, 4% v/v) and the mixture was stirred at room temperature. After 10 min, volatiles were removed in vacuo, the residue was dissolved in EtOAc (20 mL), and the solution was extracted with water (2 × 10 mL). The organic layer was discarded and the aqueous layers were lyophilized. Flash chromatography of the residue on reverse phase silica gel (H<sub>2</sub>O/CH<sub>3</sub>CN 6:4), followed by lyophilization, gave 0.19 g (0.28 mmol, 79%) of the free thiol **11** as a white fluffy solid, 205 °C (dec), R<sub>f</sub> 0.51 (H<sub>2</sub>O/CH<sub>3</sub>CN 6:4). HRMS (ESI<sup>+</sup>, *m/z*) calculated for C<sub>22</sub>H<sub>39</sub>EuN<sub>3</sub>O<sub>7</sub>S 670.1770, found 670.1777 (M + H)<sup>+</sup>.

**Preparation of Mercapt-HSA (mHSA).** To a 1.0 mM solution of HSA (5.2 g, 0.08 mmol) in 0.1 M sodium phosphate buffer (80 mL, pH 6.86) containing 0.3 M NaCl (1.4 g, 2.38 mmol) was added dithiothreitol (DTT, 62 mg, 0.4 mmol) and the mixture was stirred at rt. After 45 min, the mixture was loaded into a dialysis membrane and dialyzed at 4 °C against 0.05 M TRIS buffer (pH 7.3) for 10 days and against distilled water for 5 days. Lyophilization gave mHSA as a fluffy solid.

**Ellman's Assay of HSA.** The four types of HSA were made up as 0.67 mM solutions in PBS buffer adjusted to pH 8.0 and kept on ice until use. Ellman's reagent (DTNB) was prepared as a 4 mM stock solution in PBS buffer at pH 8.0 and kept on ice wrapped in aluminum foil until use. A 10 mM stock solution of L-cysteine (Sigma) was used as a standard and was prepared in PBS buffer at pH 8.0 and kept on ice until use. A 96-well plate was kept on ice and loaded with the various types of HSA (0.57 mM final concentration) or L-cysteine (0–0.3 mM final concentration) and DTNB (0.57 mM final concentration). The 96-well plate was then transferred to an optical absorbance plate reader and the optical absorbance at 412 nm measured at room temperature. Quadruplicate data points were determined and averaged.

**NMR Studies of Interactions between Compound 11 and HSA.** The 1D and 2D NMR experiments were carried out using a Bruker DRX600 spectrometer at 310 K. The 1D <sup>1</sup>H spectra with 9000 Hz spectral width and 8 k time domain data points were acquired using presaturation for residual water suppression. The data were zero-filled to 32 k, apodized with an optimized combination of squared-sinebell and Gaussian functions for resolution enhancement, and Fourier transformed. The 2D <sup>1</sup>H–<sup>1</sup>H spectra were usually acquired with a spectral width of 9000 Hz, 512 *t*<sub>1</sub> points, 2K data points in *t*<sub>2</sub>, and 96 or 112 transients for each *t*<sub>1</sub> point, and all 2D spectra were recorded in pure absorption with time-proportional phase incrementation (TPPI). The residual solvent resonance in D<sub>2</sub>O was suppressed by selective irradiation during the preparation period. The 2D <sup>1</sup>H–<sup>1</sup>H TOCSY experiments used a mixing time of 65 ms; a delay, 2.4 times the 90° pulse, was inserted between each pulse of each block of the MLEV-17 spin lock period. Conventional pulse sequences were used for DQF-COSY spectra. All 1D and 2D spectra were processed on a Unix computer using TopSpin 2.0 (Bruker). Prior to 2D Fourier transformation, the data were multiplied by squared sine bells in both *t*<sub>1</sub> and *t*<sub>2</sub> and zero-filled to yield a 2048 × 2048 matrix of real data points.

**Binding of Gd-thiols to HSA.** Solutions of Gd complexes **1**, **2**, and **3a–3e** were made in PBS, and in corresponding solutions that contained 0.6 mM human serum albumin from donor plasma (HSA, Sigma), recombinant HSA (rHSA, Invitria), recombinant lipid-reduced HSA (rHSA-LR, Invitria), or mercapt-HSA (mHSA) prepared from HSA obtained from Sigma, as well as 0–2.0 mM homocysteine (Sigma), to final gadolinium concentrations of 0–1.0 mM. All solutions also contained 10 mM sodium azide, and the final pH of all solutions was 7.40 ± 0.05 at room temperature. Solutions were allowed to equilibrate overnight at 37 °C under air atmosphere prior to measurements. Aliquots (500 μL) of each solution containing HSA were placed in prewarmed ultrafiltration units (Amicon Ultra-4 Centrifugal Filter Units, 30000 MW cutoff, Millipore Corporation) and immediately centrifuged at 7450 × *g* for 10.7 min, inclusive of

braking time. It was assumed that gadolinium bound to HSA (Gd<sub>bound</sub>) would not pass through the membrane and that gadolinium in the filtrate (Gd<sub>free</sub>) accurately represented the unbound gadolinium in each sample. Gadolinium concentrations in the filtrates were determined by MRI relaxometry. The apparent equilibrium binding constant (K<sub>A</sub>) for each complex was calculated from the Law of Mass Action as described previously.<sup>12</sup>

**Relaxivity of Gd Complexes in the Absence of HSA.** Measurements of the longitudinal water-proton relaxivities of Gd complexes in buffered saline were made at 37 °C on a 7 T Bruker Biospec MR Instrument (Bruker Biospin, Billerica, MA). 96-Well tissue culture plates (Falcon) were cut down to 6 × 8 wells, creating a sample tray which fit inside a 72 mm ID birdcage radio frequency transmitter-receiver coil (Bruker). Aliquots (250 μL) of the gadolinium solutions were loaded into these wells. Spaces between the wells were filled with water in order to reduce air–water susceptibility artifacts in the images. The sample tray was maintained at 37 °C during imaging by flowing heated air over the sample tray. Sample temperature was continuously monitored using a fluoroptic temperature probe (Luxtron Corporation, Santa Clara, CA). Spin-echo MR images of cross sections of the wells were acquired with recycle times (T<sub>R</sub>) ranging between 35 and 8000 ms and an echo time (T<sub>E</sub>) of 4 ms. Signal intensity *S* in each well was fitted to eq 1 to extract the T<sub>1</sub> at each solution condition. The factor *c* was between 0.99 and 1.0 in all regressions.

$$S = S_0 \left( 1 - c \times \exp \left[ \frac{-T_R}{T_1} \right] \right) \quad (1)$$

The T<sub>1</sub> relaxation times of the solutions of gadolinium in saline containing 0–2.0 mM homocysteine thus calculated were then fit to eq 2, and a longitudinal relaxivity *r*<sub>1</sub> obtained for each solution condition.

$$\frac{1}{T_1} = \frac{1}{T_{10}} + r_1 \times [\text{Gd}] \quad (2)$$

Here 1/T<sub>10</sub> is the relaxation rate in the absence of contrast agent, and [Gd] is the concentration of gadolinium in the solution.

**Relaxivity of Gd Complexes in the Presence of HSA.** The relaxivity of gadolinium in HSA-containing solutions was approximated to have only two components: “free” (monomer, homodimer, heterodimer), and “bound” (to HSA). The T<sub>1</sub> times of the solutions of gadolinium complex in saline + HSA were inserted into eq 3 and fitted for the relaxivity of bound gadolinium, *r*<sub>1,bound</sub>

$$\frac{1}{T_1} = \frac{1}{T_{10}} + r_{1,\text{free}} \times [\text{Gd}_{\text{free}}] + r_{1,\text{bound}} \times [\text{Gd}_{\text{total}} - \text{Gd}_{\text{free}}] \quad (3)$$

where Gd<sub>free</sub> was obtained as described previously<sup>10</sup> with K<sub>A</sub> constrained to equal the binding constant calculated for the respective HSA-containing solution. In these regressions, *r*<sub>1,free</sub> was constrained to equal the relaxivity measured in the corresponding HSA-free solution.

## ■ ASSOCIATED CONTENT

### Supporting Information

<sup>1</sup>H and <sup>13</sup>C NMR spectra for compounds **5a–5e**, **6a–6e**, **7a–7e**, **11**, full size 2D <sup>1</sup>H–<sup>1</sup>H NMR TOCSY spectra, and analytical RP-HPLC chromatograms for **3a–3e**. This material is available free of charge via the Internet at <http://pubs.acs.org>.

## ■ AUTHOR INFORMATION

### Corresponding Author

\*Phone (520) 626-6041; e-mail [raghunan@email.arizona.edu](mailto:raghunan@email.arizona.edu).

### Notes

The authors declare no competing financial interest.

## ACKNOWLEDGMENTS

This work was supported by grants R01-CA118359, P01-CA017094, and P30-CA023074 from the National Institutes of Health.

## ABBREVIATIONS USED

ARE, antioxidant response element; CAs, contrast agents; DCM, dichloromethane; DO3A, 1,4,7,10-tetraazacyclododecane-1,4,7-triacetic acid; DOTA, 1,4,7,10-tetraazacyclododecane-1,4,7,10-tetraacetic acid; GSH, reduced glutathione; HSA, human serum albumin; GGT,  $\gamma$ -glutamyltransferase; KEAP1, Kelch-like ECH-associated protein 1; mHSA, mercapt-human serum albumin; MRI, magnetic resonance imaging; MRP, multidrug resistance-associated protein; NPSH, non-protein thiols; NRF2, nuclear factor erythroid 2-related factor 2; PBS, phosphate-buffered saline; PEG, polyethylene glycol; rHSA, recombinant human serum albumin; rHSA-LR, recombinant lipid-reduced human serum albumin; TBAI, tetrabutylammonium iodide; TOCSY, total correlation spectroscopy

## REFERENCES

- (1) Moriarty-Craige, S. E.; Jones, D. P. Extracellular thiols and thiol/disulfide redox in metabolism. *Annu. Rev. Nutr.* **2004**, *24*, 481–509.
- (2) Hayes, J. D.; McMahon, M. NRF2 and KEAP1 mutations: permanent activation of an adaptive response in cancer. *Trends Biochem. Sci.* **2009**, *34*, 176–188.
- (3) Di Giuseppe, D.; Olivelli, M.; Bartalini, S.; Battistini, S.; Cerase, A.; Passero, S.; Summa, D.; Frosali, S.; Priora, R.; Margaritis, A.; Di Simplicio, P. Regulation of redox forms of plasma thiols by albumin in multiple sclerosis after fasting and methionine loading test. *Amino Acids* **2010**, *38*, 1461–1471.
- (4) Chen, X.; Carystinos, G. D.; Batist, G. Potential for selective modulation of glutathione in cancer chemotherapy. *Chemico-Biol. Interactions* **1998**, *111–112*, 263–275.
- (5) Ong, P. S.; Chan, S. Y.; Ho, P. C. Microarray analysis revealed dysregulation of multiple genes associated with chemoresistance to As<sub>2</sub>O<sub>3</sub> and increased tumor aggressiveness in a newly established arsenic-resistant ovarian cancer cell line, OVCAR-3/AsR. *Eur. J. Pharm. Sci.* **2012**, *45*, 367–378.
- (6) Tuttle, S.; Horan, A.; Koch, C. J.; Held, K.; Manevich, Y.; Biaglow, J. Radiation-sensitive tyrosine phosphorylation of cellular proteins: sensitive to changes in GSH content induced by pretreatment with N-acetyl-L-cysteine or L-buthionine-S,R-sulfoximine. *Int. J. Radiat. Oncol. Biol. Phys.* **1998**, *42*, 833–838.
- (7) Pei, P.; Horan, M. P.; Hille, R.; Hemann, C. F.; Schwendeman, S. P.; Mallery, S. R. Reduced nonprotein thiols inhibit activation and function of MMP-9: implications for chemoprevention. *Free Radic. Biol. Med.* **2006**, *41*, 1315–1324.
- (8) Blakytyn, R.; Erkel, L. J.; Brunner, G. Inactivation of active and latent transforming growth factor beta by free thiols: potential redox regulation of biological action. *Int. J. Biochem. Cell. Biol.* **2006**, *38*, 1363–1373.
- (9) Satoh, H.; Moriguchi, T.; Taguchi, K.; Takai, J.; Maher, J. M.; Suzuki, T.; Winnard, P. T., Jr.; Raman, V.; Ebina, M.; Nukiwa, T.; Yamamoto, M. Nrf2-deficiency creates a responsive microenvironment for metastasis to the lung. *Carcinogenesis* **2010**, *31*, 1833–1843.
- (10) Raghunand, N.; Jagadish, B.; Trouard, T. P.; Galons, J. P.; Gillies, R. J.; Mash, E. A. Redox-sensitive contrast agents for MRI based on reversible binding of thiols to serum albumin. *Magn. Reson. Med.* **2006**, *55*, 1272–1280.
- (11) Guntle, G. P.; Jagadish, B.; Mash, E. A.; Powis, G.; Dorr, R. T.; Raghunand, N. Tumor xenograft response to redox-active therapies assessed by Magnetic Resonance Imaging using a thiol-bearing DOTA complex of gadolinium. *Trans. Oncol.* **2012**, *5*, 190–199.
- (12) Raghunand, N.; Guntle, G. P.; Gokhale, V.; Nichol, G. S.; Mash, E. A.; Jagadish, B. Design, synthesis, and evaluation of 1,4,7,10-tetraazacyclododecane-1,4,7-triacetic acid derived. redox-sensitive contrast agents for magnetic resonance imaging. *J. Med. Chem.* **2010**, *53*, 6747–6757.
- (13) Ke, C.; Yang, C.; Mori, T.; Wada, T.; Liu, Y.; Inoue, Y. Catalytic enantiodifferentiating photocyclodimerization of 2-anthracenecarboxylic acid mediated by a non-sensitizing chiral metallosupramolecular host. *Angew. Chem., Int. Ed.* **2009**, *48*, 6675–6677.
- (14) Choi, J. Y.; Seo, H. N.; Lee, M. J.; Park, S. J.; Jeon, J. Y.; Kang, J. H.; Pae, A. N.; Rhim, H.; Lee, J. Y. Synthesis and biological evaluation of novel T-type calcium channel blockers. *Bioorg. Med. Chem. Lett.* **2007**, *17*, 471–475.
- (15) Alisi, M. A.; Brufani, M.; Filocomo, L.; Gostoli, G. Synthesis and structure-activity relationships of new acetylcholinesterase inhibitors: morpholinoalkyl carbamoyloxyseryl derivatives. *Bioorg. Med. Chem. Lett.* **1995**, *5*, 2077–2080.
- (16) Sengupta, S.; Chen, H.; Togawa, T.; DiBello, P. M.; Majors, A. K.; Budy, B.; Ketterer, M. E.; Jacobsen, D. W. Albumin thiolate anion is an intermediate in the formation of albumin-S-S-homocysteine. *J. Biol. Chem.* **2001**, *276*, 30111–30117.
- (17) Ellman, G. L. Tissue sulfhydryl groups. *Arch. Biochem. Biophys.* **1959**, *82*, 70–77.
- (18) Takeda, K.; Shigemura, A.; Hamada, S.; Gu, W.; Fang, D.; Sasa, K.; Hachiya, K. Dependence of reaction rate of 5,5'-dithiobis-(2-nitrobenzoic acid) to free sulfhydryl groups of bovine serum albumin and ovalbumin on the protein conformations. *J. Protein Chem.* **1992**, *11*, 187–192.
- (19) Christodoulou, J.; Sadler, P. J.; Tucker, A. <sup>1</sup>H NMR of albumin in human blood plasma: drug binding and redox reactions at Cys<sup>34</sup>. *FEBS Lett.* **1995**, *376*, 1–5.
- (20) Stewart, A. J.; Blindauer, C. A.; Berezenko, S.; Sleep, D.; Tooth, D.; Sadler, P. J. Role of Tyr<sup>84</sup> in controlling the reactivity of Cys<sup>34</sup> of human albumin. *FEBS J.* **2005**, *272*, 353–362.
- (21) Kragh-Hansen, U.; Chuang, V. T. C.; Otagiri, M. Practical aspects of the ligand-binding and enzymatic properties of human serum albumin. *Biol. Pharm. Bull.* **2002**, *25*, 695–704.
- (22) Bohndiek, S. E.; Kettunen, M. I.; Hu, D. E.; Kennedy, B. W.; Boren, J.; Gallagher, F. A.; Brindle, K. M. Hyperpolarized [1-<sup>13</sup>C]-ascorbic and dehydroascorbic acid: vitamin C as a probe for imaging redox status in vivo. *J. Am. Chem. Soc.* **2011**, *133*, 11795–11801.
- (23) Ratnakar, S. J.; Viswanathan, S.; Kovacs, Z.; Jindal, A. K.; Green, K. N.; Sherry, A. D. Europium(III) DOTA-tetraamide Complexes as Redox-Active MRI Sensors. *J. Am. Chem. Soc.* **2012**, *134*, 5798–5800.
- (24) Digilio, G.; Menchise, V.; Gianolio, E.; Catanzaro, V.; Carrera, C.; Napolitano, R.; Fedeli, F.; Aime, S. Exofacial protein thiols as a route for the internalization of Gd(III)-based complexes for MRI cell labelling. *J. Med. Chem.* **2010**, *53*, 4877–4890.
- (25) Menchise, V.; Digilio, G.; Gianolio, E.; Cittadino, E.; Catanzaro, V.; Carrera, C.; Aime, S. In vivo labeling of B16 melanoma tumor xenograft with a thiol-reactive gadolinium based MRI contrast agent. *Mol. Pharmaceutics* **2011**, *8*, 1750–1756.
- (26) Inner-sphere relaxation refers to relaxation enhancement of a water molecule directly coordinated to the gadolinium. Second-sphere relaxation occurs when water molecules in the second coordination sphere (H-bonded to atoms on the complex) are relaxed via a dipolar mechanism. Outer-sphere relaxation arises from the translational diffusion of water molecules near the Gd(III) complex.
- (27) Caravan, P.; Ellison, J. J.; McMurry, T. J.; Lauffer, R. B. Gadolinium(III) chelates as MRI contrast agents: structure, dynamics and applications. *Chem. Rev.* **1999**, *99*, 2293–2352.
- (28) Barge, A.; Cravotto, G.; Gianolio, E.; Fedeli, F. How to determine free Gd and free ligand in solution of Gd chelates. A technical note. *Contrast Media Mol. Imaging* **2006**, *1*, 184–188.